Analysis of the Scattering of 40-MeV Protons*†

M. P. FRICKE‡
University of Minnesota, Minneapolis, Minnesota

AND

G. R. SATCHLER
Oak Ridge National Laboratory, Oak Ridge, Tennessee

(Received 29 March 1965)

Elastic and inelastic scattering of unpolarized 40-MeV protons from ^{12}C, ^{54}Fe, ^{56}Fe, ^{58}Ni, ^{60}Ni, and ^{208}Pb have been analyzed using the optical-model potential and its collective-model extension in the distorted-wave approximation. Fits to the inelastic scattering from ^{24}Mg and to the elastic scattering from ^{27}Al, ^{65}Cu, Sn, and ^{181}Ta also are included. The Woods-Saxon shape parameters for the potential differ from those suggested for scattering at lower energies, and either surface or volume forms of the imaginary part produce good agreement with the data. To describe the inelastic scattering best, it is found necessary to deform the imaginary (as well as the real) part of the central potential. The deformation parameters obtained are in reasonable agreement with those found by other methods.

I. INTRODUCTION

NUMEROUS analyses have been made recently of the elastic[1,2] and inelastic[2] scattering of protons of energies 9 to 22 MeV, using the optical model and its collective-model generalization. The latter introduces nonspherical optical potentials. When treated to lowest order in the deformation,[2,3] the spherical part gives the elastic scattering, and the nonspherical part induces the inelastic scattering which is computed by the distorted-wave method.[4] Similar analyses have been successfully applied to the scattering of neutrons, deuterons, alpha particles, and heavy ions.

The present paper extends this analysis to protons of 40-MeV energy. Elastic scattering data[5] for Fe, Ni, and Cu, and inelastic scattering data[6] for C, Mg, Fe, Ni, and Pb are studied. Comparisons with elastic data[7] for C, Al, Sn, Ta, and Pb are also given.

* Research jointly sponsored by the U. S. Atomic Energy Commission under contract with the Union Carbide Corporation and the University of Minnesota.

† Preliminary results of this work were submitted by one of us (MPF) in partial fulfillment of the requirements for an M. S. degree, University of Minnesota, and have been reported in *Nuclear Spectroscopy with Direct Reactions, I: Contributed Papers*, Argonne National Laboratory Report No. ANL-6848, 1964 (unpublished).

‡ Presently ORINS Graduate Fellow at Oak Ridge National Laboratory.

[1] F. G. Perey, Phys. Rev. **131**, 745 (1963).

[2] B. Buck, Phys. Rev. **130**, 712 (1963); G. R. Satchler, R. H. Bassel, and R. M. Drisko, Phys. Letters **5**, 256 (1963); M. Sakai, H. Ikegami, Y. Nakagima, K. Yagi, H. Ejiri, and G. R. Satchler, *ibid.* **8**, 197 (1964); H. O. Funsten, N. R. Roberson, and E. Rost, Phys. Rev. **134**, B117 (1964); J. K. Dickens, F. G. Perey, R. J. Silva, and T. Tamura, Phys. Letters **6**, 53 (1963); F. G. Perey, R. J. Silva, and G. R. Satchler, *ibid.* **4**, 25 (1963); and T. Tamura (to be published).

[3] This is discussed, for example, by E. Rost and N. Austern, Phys. Rev. **120**, 1375 (1960); R. H. Bassel, G. R. Satchler, R. M. Drisko, and E. Rost, *ibid.* **128**, 2693 (1962).

[4] G. R. Satchler, Nucl. Phys. **55**, 1 (1964), and other references given there.

[5] M. K. Brussel and J. H. Williams, Phys. Rev. **114**, 525 (1959).

[6] T. Stovall and N. M. Hintz, Phys. Rev. **135**, B330 (1964). This paper includes some comparisons with experiment of the preliminary results of the present analysis using real coupling.

[7] M. K. Brussel, N. M. Hintz, and J. H. Williams, University of Minnesota Linear Accelerator Annual Progress Report, 1956-1957 (unpublished). See also, A. E. Glassgold and P. J. Kellogg, Phys. Rev. **109**, 1291 (1958).

II. THEORY

The elastic scattering is described with an eight-parameter optical potential,

$$U(r)=-V(e^x+1)^{-1}-i(W-4W_D d/dx')(e^{x'}+1)^{-1}+(\hbar/m_\pi c)^2 V_S\,\boldsymbol{\sigma}\cdot\mathbf{l}(1/r)(d/dr)(e^x+1)^{-1},$$
$$x=(r-r_0A^{1/3})/a,\quad x'=(r-r_0'A^{1/3})/a',\qquad(1)$$

to which is added the Coulomb potential for a uniformly charged sphere of radius $1.2A^{1/3}$ F. For the present analysis of unpolarized proton scattering, the spin-orbit term has been taken to be real with a radial shape given by the derivative of that for the real, central term. Indeed, there is as yet no convincing evidence that a complex spin-orbit coupling is required even to explain the observed polarizations at 40 MeV.

It is shown in what follows that good fits to the data are obtained with either pure surface absorption ($W=0$) or pure volume absorption ($W_D=0$), so that two forms of the potential, each with seven parameters, are found successful.

The parameters which best fit the elastic scattering were determined by use of an automatic search routine[8] which minimizes the quantity

$$\chi^2=(1/N)\sum_{i=1}^{N}\{[\sigma_{\mathrm{TH}}(\theta_i)-\sigma_{\mathrm{EX}}(\theta_i)]/\Delta\sigma_{\mathrm{EX}}(\theta_i)\}^2,\qquad(2)$$

where $\sigma_{\mathrm{EX}}(\theta_i)$ is the measured, and $\sigma_{\mathrm{TH}}(\theta_i)$ the calculated, differential cross section at angle θ_i, while $\Delta\sigma_{\mathrm{EX}}$ is the "error," or weight, associated with σ_{EX}.

The results presented here were obtained by analysis of the cross sections alone and do not necessarily give the best fit to the polarization in the cases where this has been measured. Studies are in progress in which simultaneous fits to cross sections and polarizations are made by extending the definition (2) of χ^2 in an obvious way to include polarization.[9] Experience to date has been that quite small readjustments of the parameters are required to account for the measured polarizations.

The inelastic scattering is described using first-order

[8] R. M. Drisko (unpublished).

[9] E. Adams and R. M. Haybron (private communication).

distorted-wave theory[3,4] and assuming the collective-model generalization of the optical model.[2,3] The collective-model interaction form factor for excitation of a 2^l-pole rotation or single-phonon surface oscillation is obtained by deforming the central part of the optical potential. When only the real well is deformed, the form factor of this interaction, calculated to first order in the deformation, has the radial dependence[3]

$$f(r)=r_0(d/dr)[V(e^x+1)^{-1}]. \quad (3)$$

For the present calculations, however, it was found necessary to deform also the imaginary part of the potential. In this case, a complex-valued form factor is obtained which has the radial dependence $f(r)+ig(r)$, where

$$g(r)=r_0'(d/dr)\{[W-4W_D(d/dx')](e^{x'}+1)^{-1}\} \quad (4)$$

if the same deformation is assumed for both real and imaginary potentials. This "complex-coupling" model has been successful in other analyses of proton,[2] deuteron, and alpha[10] scattering. It will be noticed that the imaginary part of the coupling form factor (4) is proportional to the first derivative of the Saxon-Woods shape for volume absorption ($W_D=0$), and the second derivative for surface absorption ($W=0$). Despite this difference in shape, the two forms give very similar results. Indeed, in one previous analysis[11] it was found necessary to include this imaginary part of the coupling in order that a surface- and a volume-absorbing potential, which gave very similar elastic scattering, should also give similar inelastic scattering.

This model also assumes that the interaction producing the excitation is independent of the proton spin. The possibility of transferring angular momentum to the nucleus by spin-flip of the scattered proton is neglected, so the angular-momentum transfer is equal to l, the multipole order.[4] [The parity change $(-)^l$ is also determined by l.] The differential cross sections for spin-flip transitions are expected to be very similar to those calculated without spin-flip, so that shape alone is not a clue to the possible importance of spin-flip. However, without spin-flip a first-order excitation of an even spin-zero nucleus is restricted to "normal" parity states; that is, those whose parity π and spin j are related by $\pi=(-)^j$ because $j=l$ in this case. Spin-flip allows $j=l\pm1$ as well as $j=l$, and hence the excitation of non-normal parity states. Little information is available on the excitation of such states by protons. The polarization of the inelastic protons could be expected to be more sensitive to the presence of spin-flip in $j=l$ transitions, and measurements of this would be useful. Some discussion and illustration of inelastic polarization has been given in the M.S. thesis of one of us (MPF) where the results of calculations with real coupling but no spin-flip are presented. In particular, it was found that the polarization-asymmetry equality which holds exactly for elastic scattering is also obeyed to a good approximation by the inelastic-scattering calculations. Further studies of the polarization have been initiated.

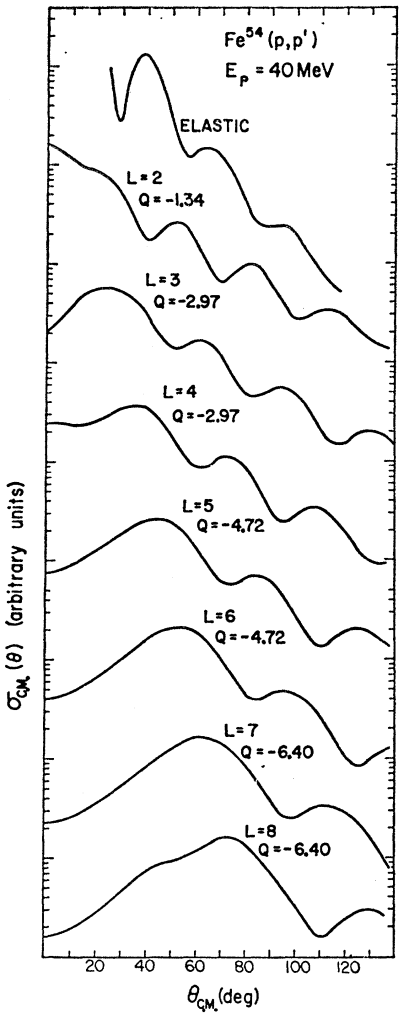

FIG. 1. Typical predictions for various multipole excitations in ^{54}Fe, showing sensitivity to multipolarity l. Typical Q values were assumed, although the scattering is relatively insensitive to the value used.

Apart from the strengths, or deformation parameters β_l,[3] of the multipole components of deformation, the parameters for the inelastic scattering are completely determined in this model by the fits to the elastic scattering. (It is assumed that the same optical potential may be used in both exit and entrance channels.) The angular distributions are the same for vibrations or rotations; their magnitude is proportional to β_l^2, and their shape is independent of β_l. Figure 1 shows a set of predicted differential cross sections for $l=2$ through 8 for ^{54}Fe and a set of typical Q values. These were calculated using real coupling only, but for the illustrative purposes of this figure the effect of complex coupling is

[10] H. W. Broek, J. L. Yntema, and G. R. Satchler, Nucl. Phys. **64**, 259 (1964).

[11] K. Yagi, H. Ejiri, M. Furukawa, Y. Ishizaki, M. Koike, K. Matsuda, Y. Nakajima, I. Nonaka, Y. Saji, E. Tanaka, and G. R. Satchler, Phys. Letters **10**, 186 (1964).

unimportant. Remnants can be seen in this figure of the Blair phase rule[12] for odd and even l, in the sense that the oscillations in the angular distribution show a regular phase shift as l increases. However the departures from the simple phase rule are much more marked than for, say, high-energy alpha particles.[3,12]

When the deformation is large, multiple excitations between the ground and excited states may become important, in which case the scattering must be calculated to higher order than is done here. To some extent, however, the corrections are accounted for empirically in the present method, since the optical-model parameters are adjusted to reproduce the observed elastic scattering.[13] To test the situation for these 40-MeV data, coupled-equation calculations[14] were made for the states in ^{12}C and ^{58}Ni. The same optical-model parameters were used as in the distorted-wave calculations. No significant difference from the first-order theory was found.

The inelastic-scattering calculations include Coulomb-excitation amplitudes derived in the manner of Ref. 3. For the medium-weight nuclei, these affected only the normalization of the calculated angular distributions, increasing β_2 by about 10% and β_3 by less than 5%. The angular distributions show some slight interference structure at very forward angles, but data are not available in this region.

The potentials used in the present work are taken to be local. We have good reason to believe the optical potential is nonlocal, but it is known that, at a given energy, a local potential can be found to give the same elastic scattering.[15] The wave function associated with the nonlocal potential, however, is reduced in amplitude in the nuclear interior compared to that for the local potential.[16] Further, when the potential is deformed, the inelastic coupling interaction also becomes nonlocal. Both these nonlocality effects can be studied in the local-energy approximation,[17] and it has been shown that they lead to small ($\sim$20%) reductions in the predicted cross sections.[18] Hence, the deformations β_l deduced in the present paper using local potentials may be underestimated by about 10%.

III. RESULTS AND DISCUSSION

1. Elastic Best Fits

Initial attempts to fit the elastic scattering from ^{58}Ni using the values suggested by Perey[1] for the "geometrical" parameters (namely, $r_0=r_0'=1.25$ F, $a=0.65$ F and $a'=0.47$ F) were unsuccessful, even when both volume and surface absorption were included. However, good agreement with all of the iron, nickel, and lead elastic data could be achieved by allowing these parameters to vary substantially from those values found adequate at the lower energies. Also, equally good fits could be obtained with surface ab-

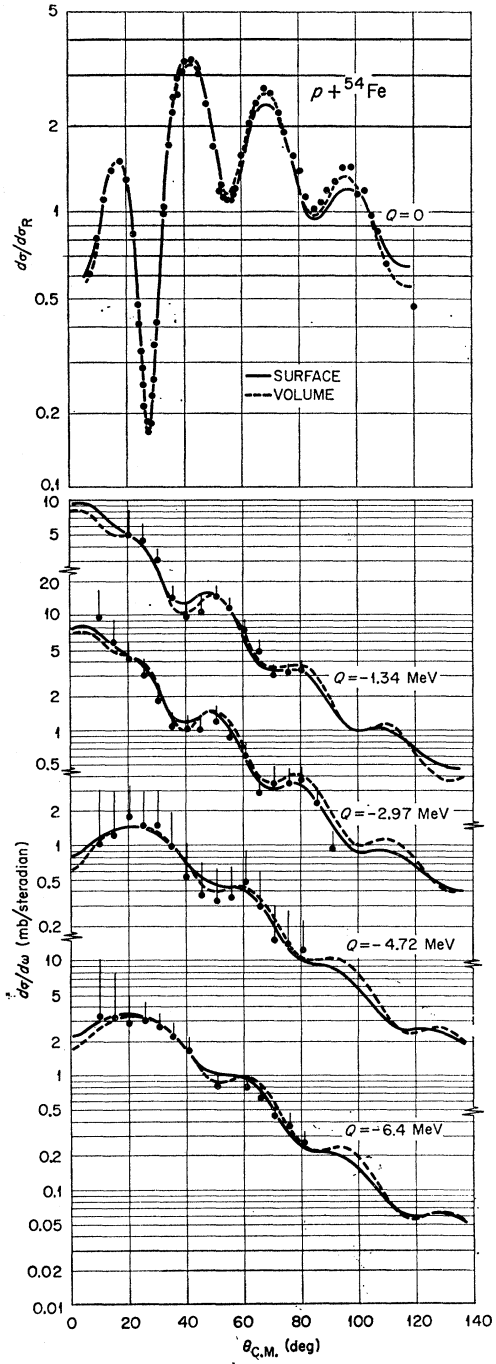

FIG. 2. The elastic and inelastic scattering calculated for both surface and volume forms of absorption, compared to measured cross sections for ^{54}Fe. The inelastic-scattering calculations use complex coupling and include contributions from Coulomb excitation. The parameters used are listed in Tables I and II.

[12] J. S. Blair, Phys. Rev. **115**, 928 (1959).
[13] F. G. Perey and G. R. Satchler, Phys. Letters **5**, 212 (1963).
[14] The code of B. Buck (Ref. 2) was used for these; see also B. Buck, Phys. Rev. **127**, 940 (1962).
[15] F. G. Perey and B. Buck, Nucl. Phys. **32**, 353 (1962).
[16] F. G. Perey, in *Proceedings of Conference on Direct Interactions and Nuclear Reaction Mechanisms*, edited by E. Clementel and C. Villi (Gordon and Breach Science Publishers, Inc., London, 1963); N. Austern, Phys. Rev. **137**, B752 (1965).
[17] F. G. Perey and D. S. Saxon, Phys. Letters **10**, 107 (1964).
[1] F. G. Perey and A. M. Saruis, Nucl. Phys. (to be published).

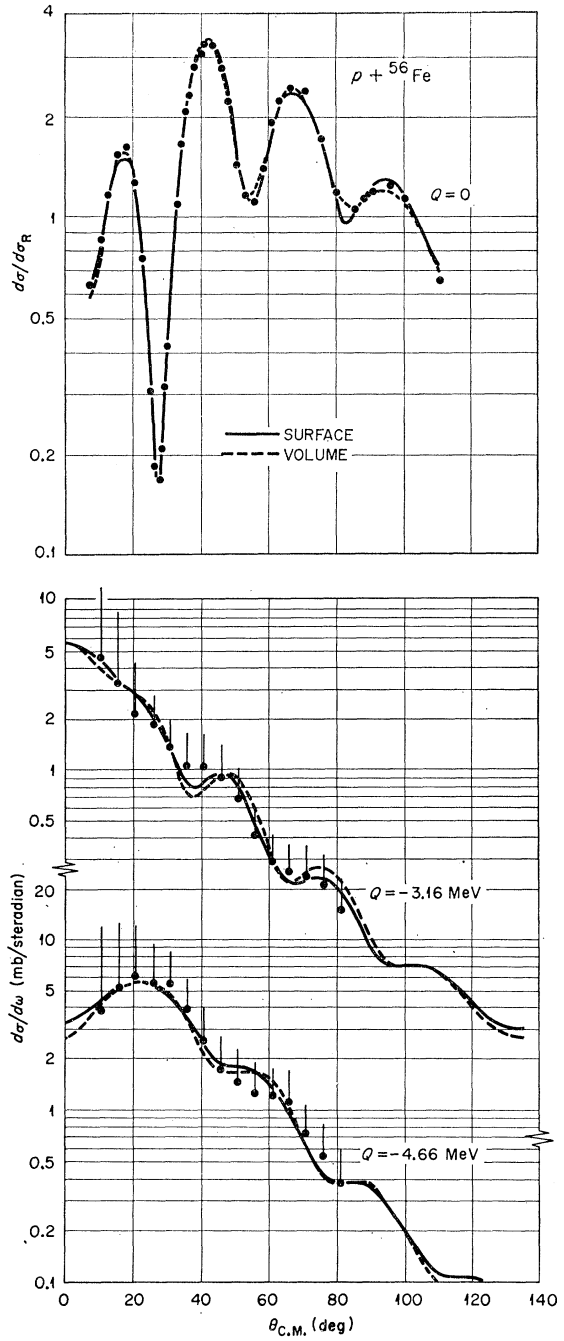

FIG. 3. Scattering from ^{56}Fe (see caption of Fig. 2).

sorption, volume absorption, or a mixture of both. Since the latter form of the potential has one more parameter than the others, it was not used in subsequent calculations. Even though there are grounds for believing the true absorptive potential has both surface and volume components, analyses of the present data are apparently unable to reveal their relative strengths. This situation seems to hold even at 55-MeV energy,[11] but analyses of 182-MeV data[19] show an unmistakable preference for volume absorption.

Figures 2 through 6 show comparisons of the theoretical curves with the measured cross sections obtained for Fe, Ni, and Pb. Surface- and volume-absorption potentials were used whose seven parameters were all varied to fit the elastic data. Very good agreement with experiment is seen. Particularly remarkable is the very deep minimum around 30° in the elastic cross sections for Fe and Ni. Probable errors of the measured cross sections are, on the average, less than 8%.

The optical-model parameters found, and their

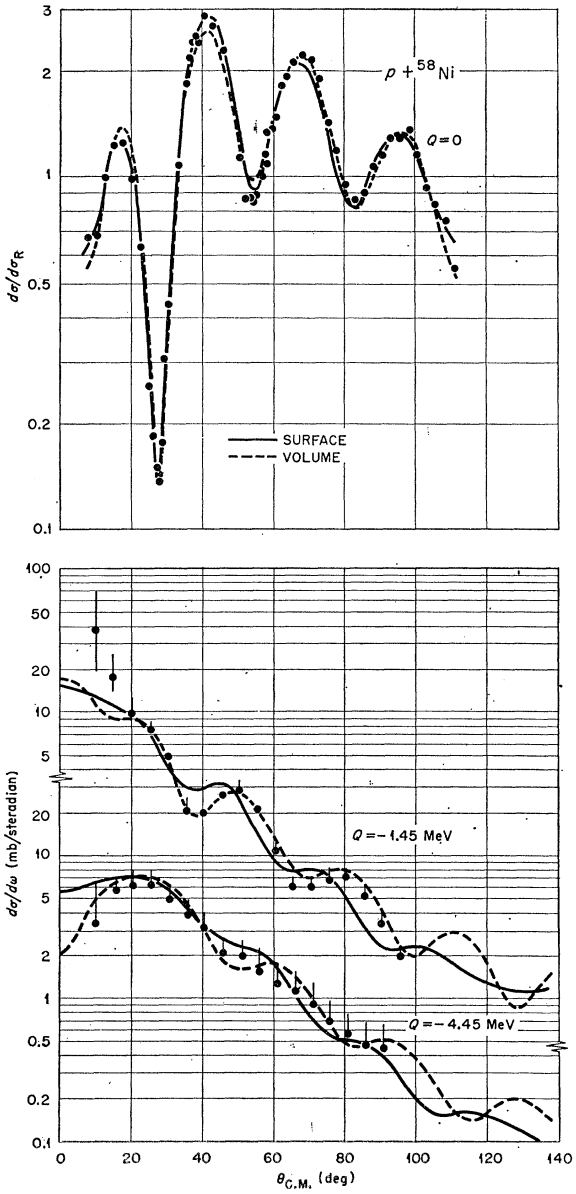

FIG. 4. Scattering from ^{58}Ni (see caption of Fig. 2).

[19] G. R. Satchler and R. M. Haybron, Phys. Letters **11**, 313 (1964).

corresponding reaction cross sections, are listed in Table I. Within 5% the reaction cross sections are the same for surface and volume absorption. Parameters for ^{65}Cu are given also; fits to these data are similar in quality to those shown for Fe, Ni, and Pb. The quantity χ^2 is given with each set of values. For calculating this, the experimental "errors" $\Delta\sigma$ were taken to be 5% at all angles; the number N of data points ranged between 40 and 64.

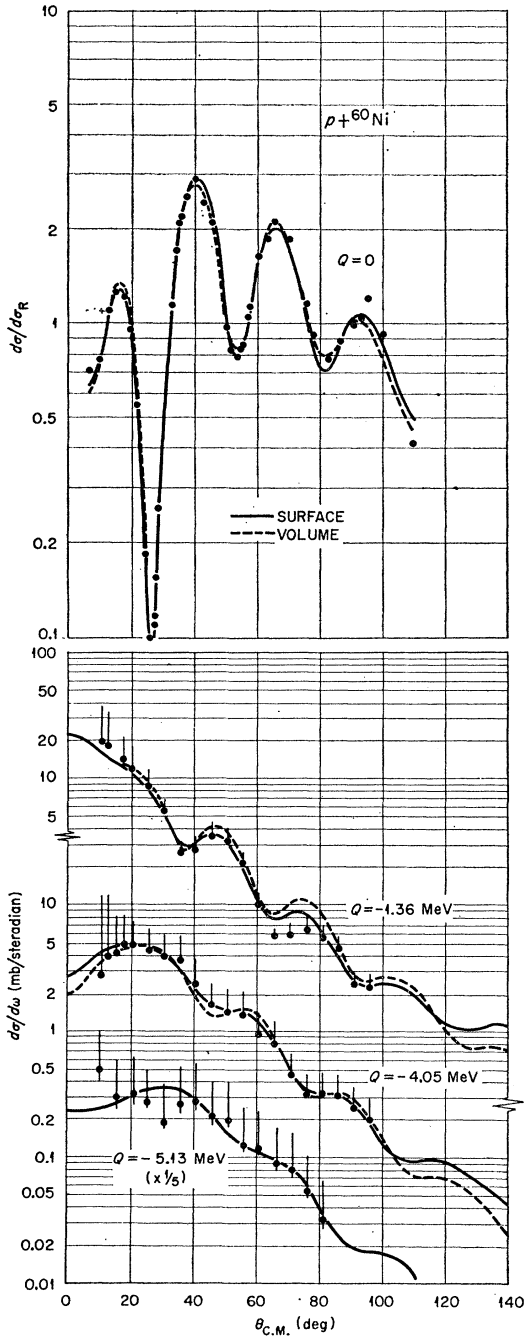

FIG. 5. Scattering from ^{60}Ni (see caption of Fig. 2).

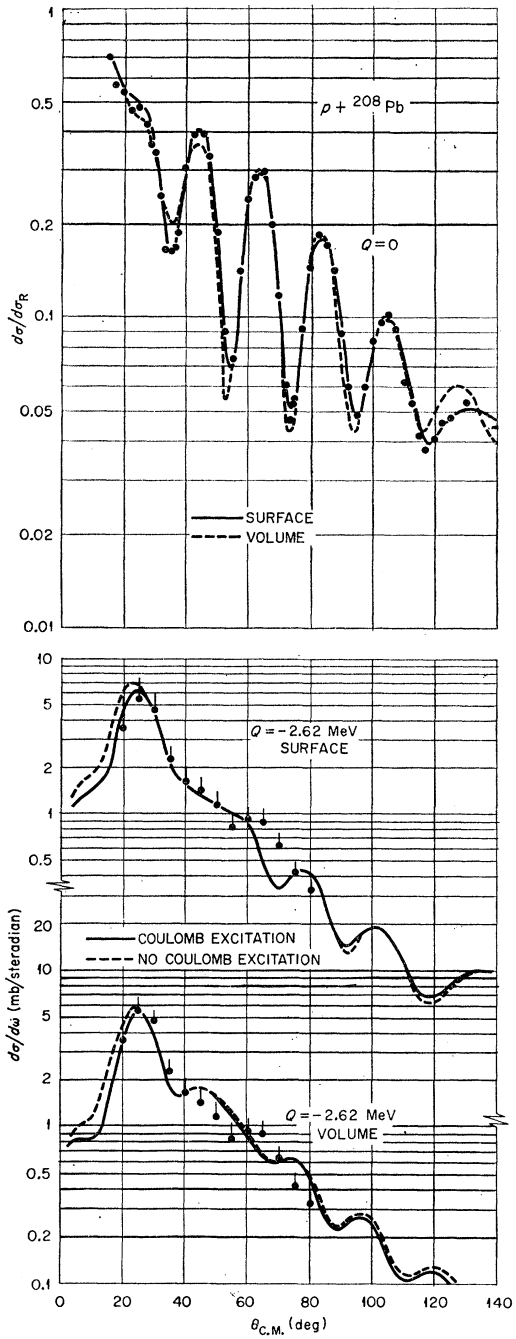

FIG. 6. Scattering from ^{208}Pb. The inelastic scattering is calculated using complex coupling both with and without contributions from Coulomb excitation (the same value for β_3 is used in each case). The parameters are given in Tables I and II.

The total reaction cross sections are in general agreement with what data exist. Gooding's[20] value for Fe at 34 MeV is 902 mb, and Meyer *et al.*[21] find 617 mb for

[20] T. J. Gooding, Nucl. Phys. **12**, 241 (1959).
[21] V. Meyer, R. M. Eisberg, and R. F. Carlson, Phys. Rev. **117**, 1334 (1960).

TABLE I. Optical-model parameters and calculated reaction cross sections for "best-fit" surface ($W=0$) and volume ($W_D=0$) potentials with variable shape parameters.

Nucleus	V (MeV)	W (MeV)	W_D (MeV)	V_s (MeV)	r_0 (F)	r_0' (F)	a (F)	a' (F)	σ_R (mb)	χ^2
^{54}Fe	44.8	8.1	0	6.51	1.169	1.403	0.755	0.441	938	1.34
^{54}Fe	45.9	0	8.7	7.40	1.164	1.043	0.694	0.695	940	3.09
^{56}Fe	43.5	6.5	0	6.37	1.173	1.451	0.736	0.758	1055	1.04
^{56}Fe	44.3	0	7.6	7.43	1.180	1.028	0.703	0.805	1015	1.54
^{58}Ni	39.6	9.6	0	4.50	1.251	1.387	0.760	0.254	986	2.67
^{58}Ni	44.5	0	10.8	10.3	1.165	1.027	0.747	0.604	957	1.85
^{58}Ni	42.7	1.5	10.3	7.67	1.211	1.067	0.707	0.545	959	2.09
^{60}Ni	44.3	7.1	0	6.52	1.165	1.459	0.755	0.594	1067	2.17
^{60}Ni	44.7	0	9.9	7.54	1.184	1.056	0.707	0.653	1021	1.89
^{65}Cu	44.4	6.3	0	7.90	1.150	1.535	0.777	0.779	···	3.80
^{65}Cu	44.9	0	9.9	7.52	1.163	0.973	0.806	0.818	1165	2.89
^{208}Pb[a]	51.0	8.0	0	6.6	1.20	1.428	0.65	0.704	2043	6.10
^{208}Pb	49.0	0	18.1	5.7	1.207	1.230	0.769	0.551	1975	1.22

[a] V, r_0 and a were held fixed for this search.

Fe at 61 MeV; Turner *et al.*[22] report 1140 mb for ^{56}Fe at 30 MeV. The value for ^{56}Fe calculated here is about 1035 mb. Waddell *et al.*[23] report 1023 mb for Ni at 29 MeV, while Turner finds 1038 mb for ^{58}Ni and 1053 mb for ^{60}Ni at 30 MeV; the value found here is about 980 mb for ^{58}Ni and 1040 mb for ^{60}Ni. Turner's value for ^{208}Pb at 30 MeV is 1865 mb; Gooding's value at 34 MeV is 1775 mb; and Meyer's value at 61 MeV is 1490 mb. Our result is about 2000 mb. When roughly normalized to the nuclear area by dividing the reaction cross section by $A^{2/3}$, Gooding's data from C, Al, Fe, Sn, and Pb at 34 MeV give values of $\sigma_R/A^{2/3}$ from 51 to 85 mb. Meyer's data from the same nuclei at 61 MeV give values from 38 to 44 mb. Waddell's data from C, Al, Ni, Ag, and Au at 29 MeV fall between 65 and 86 mb; and Turner's values for Ca, Fe, Co, Ni, Sn, and Pb at 30 MeV lie between 53 and 78 mb. The present results at 40 MeV give values of $\sigma_R/A^{2/3}$ ranging from 56 to 72 mb.

For these potentials, obtained by adjusting all parameters, the real-well depths V do not increase with the asymmetry,[1] or neutron-excess parameter $\epsilon=(N\text{-}Z)/A$. This is also true for "reduced" strengths V_R, adjusted to an average radius parameter by requiring $V_R(1.18)^2=Vr_0^2$. Indeed, these V_R show an almost linear *decrease* with increasing ϵ, with a coefficient of -24 MeV. We return to this point below.

The central parts of the two types of potential are shown in Fig. 7 for typical cases. The real wells are almost identical for the two forms of absorption, and the "outer faces" of the imaginary wells are very similar, say for $r\gtrsim 5$ F. This suggests that the scattering at these energies is rather insensitive to the degree of absorption in the nuclear interior, if sufficient absorption is provided in the surface region. It does *not* mean that protons do not penetrate to the interior; the optical-model wave functions inside the potential well are not small. Similar features are shown by the potentials which give the best fit to the scattering of 17-MeV protons.[1]

2. Inelastic Scattering

Figures 2 through 6 also show the inelastic scattering for Fe, Ni, and Pb. The experimental errors are as indicated. The theoretical curves shown were calculated[24] with complex coupling using the "best-fit" potentials of Table I (including, of course, the spin-orbit coupling). With the exception of ^{58}Ni, which will receive further comment below, the inelastic scattering calculated for levels in these nuclei was also insensitive to the type of absorption. For volume absorption, oscillations in the angular distributions are slightly more pronounced, but not by an amount large enough to be distinguished in a comparison with the data. There was, however, a consistent discrepancy between the over-all slopes of the experimental angular distributions and those predicted with the real-coupling model. In every case, better agreement was achieved with complex coupling

Figure 8 shows a typical example of the difference in inelastic scattering calculated with real and complex coupling. The principle effect of adding the imaginary part is to rotate the angular distribution clockwise, while keeping the positions of the peaks approximately the same. We note that this effect could not be achieved by small variations in the shape of the real-valued form factor, i.e., by varying the radius and diffuseness parameters in Eq. (3) from the values which fit the elastic data.

Although there is only a small improvement in fit obtained for any particular case when complex coupling is used, it appears so consistently for different excited states and different nuclei that we feel it provides additional strong support for deforming both real and imaginary potentials. Of course, the effects are suffi-

[22] J. F. Turner, B. W. Ridley, P. E. Cavanagh, G. A. Gard, and A. G. Hardacre, Nucl. Phys. 58, 509 (1964).

[23] C. N. Waddell, M. Q. Makino, and R. M. Eisberg, Bull. Am. Phys. Soc. 8, 485 (1963).

[24] The code "JULIE" of R. M. Drisko (unpublished) was used.

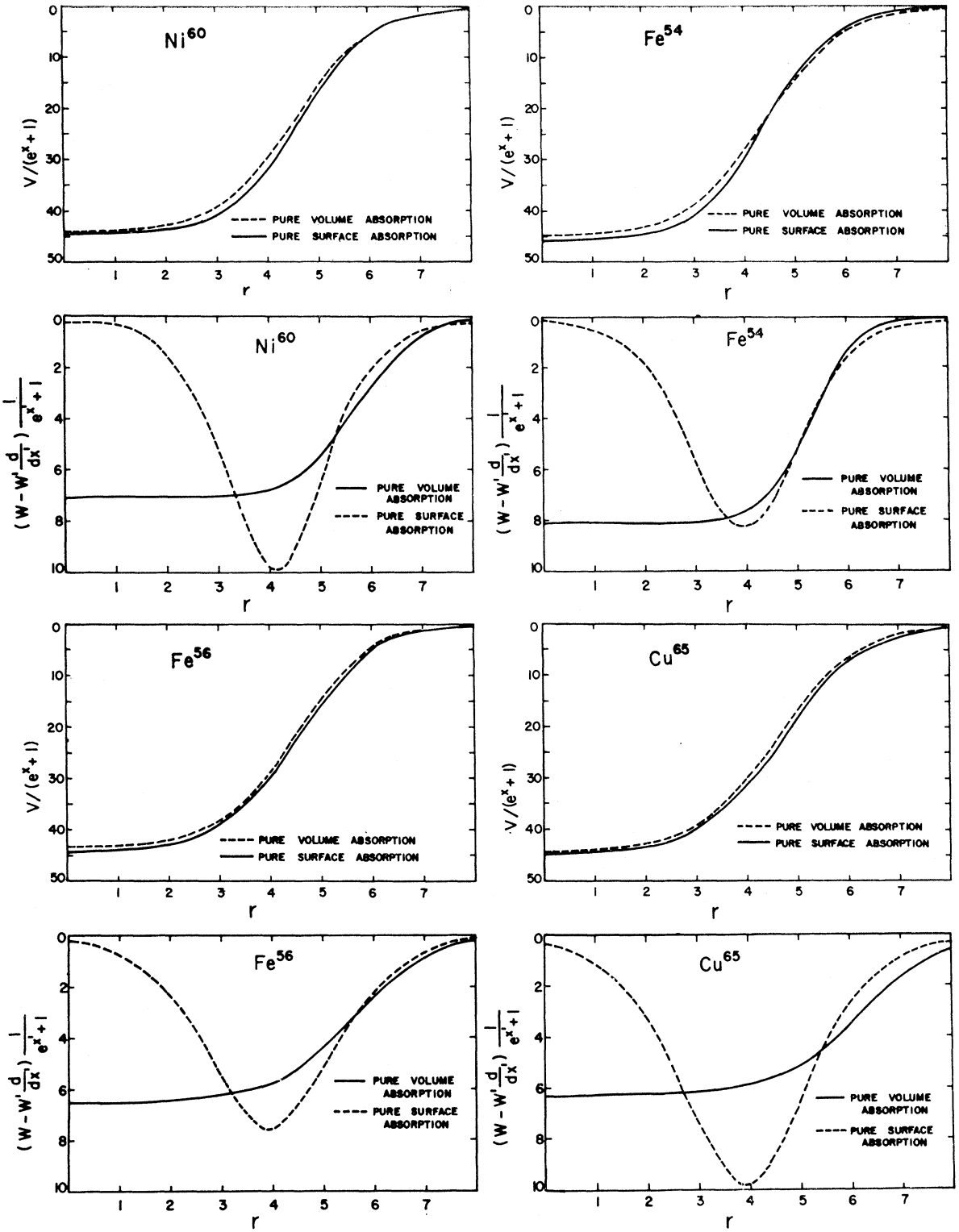

FIG. 7. Plots of the radial dependence of the central parts of some of the two types of optical potentials presented in Table I, here, $W'=4W_D$.

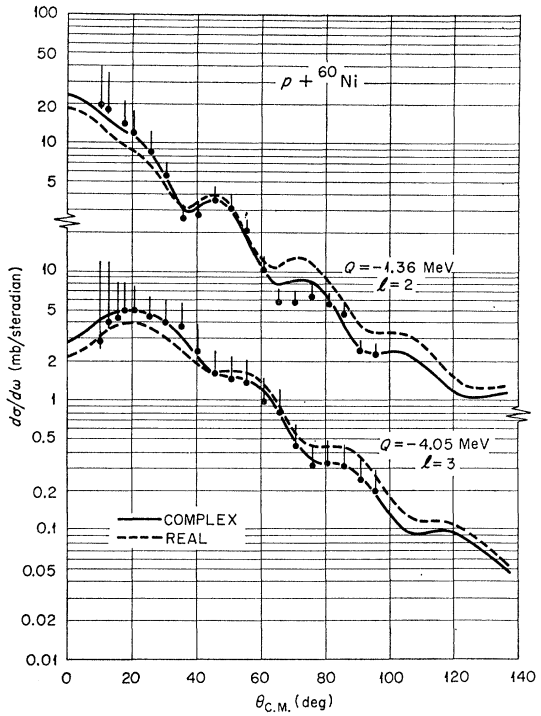

FIG. 8. Typical difference between real- and complex-coupling calculations of quadrupole and octupole inelastic scattering for medium-weight nuclei. The real form-factor curve shown has a 5% larger β_l than does the complex form-factor curve.

ciently small that it is not possible to deduce how closely the deformations of the two parts are the same.

Figure 6 also shows the effect of including Coulomb excitation for the octupole transition in Pb. It is seen that even for this heavy nucleus the effects are quite small. Coulomb excitation was included in the curves shown for the lighter nuclei Fe and Ni, but here the effects are smaller. Coulomb excitation resulted in a small and almost uniform decrease in cross section, so that the β_l required are about 10% larger for $l=2$, and less than 5% larger for $l=3$, than when it is neglected.

The values of the deformations used for the theoretical curves in Figs. 2 through 6 are given in Table II. Aside from the experimental errors for the inelastic cross sections, it is believed that the uncertainty in these β values which arises from fitting to the data is no more than about 10%. The values obtained here agree quite well with those deduced by other means (see Ref. 6, for example, for a summary of these).

TABLE II. Parameters for inelastic-scattering curves shown in figures, calculated using complex coupling and including Coulomb excitation. "Best" values are those for the potentials of Table I; "Av" values are those for the average potentials of Table III.

Nucleus	$-Q$(MeV)	l	β_l Best	β_l Av
^{12}C	4.43	2	...	0.60
^{12}C	7.66	0	...	0.12
^{12}C	9.63	3	...	0.44
^{24}Mg	1.37	2	...	0.47
^{54}Fe	1.34	2	0.15	0.15
^{54}Fe	2.97	2	0.15	0.15
^{54}Fe	4.72	3	0.10	0.10
^{54}Fe	6.4	3	0.16	0.15
^{56}Fe	3.16	2	0.11	0.11
^{56}Fe	4.66	3	0.18	0.18
^{58}Ni	1.45	2	0.19	0.19
^{58}Ni	4.45	3	0.21	0.19
^{60}Ni	1.36	2	0.22	0.21
^{60}Ni	4.05	3	0.17	0.17
^{60}Ni	5.13	4	0.13	...
^{208}Pb	2.62	3	0.11	0.11

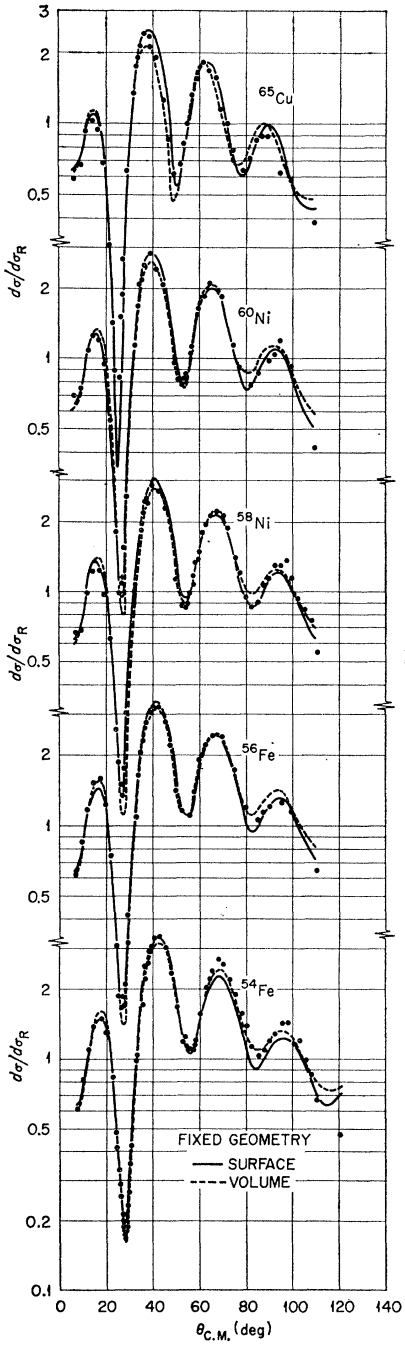

FIG. 9. Fits to elastic scattering from Fe, Ni, and Cu using potentials with the "average geometry." The calculations are made for both surface and volume forms of absorption with the parameters given in Table III.

TABLE III. Optical-model parameters and reaction cross sections for "average" surface ($W=0$) and volume ($W_D=0$) potentials with fixed geometrical parameters.

	Type of potential							
	Surface $r_0=1.18$ F, $a=0.7$ F, $r_0'=1.04$ F, $a'=0.7$ F, $V_s=7.5$ MeV				Volume $r_0=1.18$ F, $a=0.7$ F, $r_0'=1.40$ F, $a'=0.7$ F, $V_s=7.5$ MeV			
Nucleus	V (MeV)	W_D (MeV)	σ_R (mb)	χ^2	V (MeV)	W (MeV)	σ_R (mb)	χ^2
^{12}C	38.5	4.03	303	10.5	37.6	5.2	309	6.31
^{27}Al	42.3	7.25	648	6.96	39.7	7.04	638	2.64
^{54}Fe	44.5	8.68	955	4.13	42.5	7.35	992	4.58
^{56}Fe	44.9	8.80	981	1.90	42.9	7.44	1024	5.45
^{58}Ni	44.6	8.53	977	2.82	42.7	7.27	1028	5.38
^{60}Ni	44.6	9.33	1030	2.22	42.7	7.87	1085	6.95
^{65}Cu	45.4	10.5	1116	12.8	45.1	9.45	1217	14.1
Sn	49.2	13.3	1504	19.0	46.3	9.52	1636	10.9
^{181}Ta	51.2	11.9	1682	43.7	49.3	8.11	1888	28.7
^{208}Pb	54.5	13.0	1789	21.4	51.3	8.58	2015	7.40

There is some uncertainty over the identification of the 5.13-MeV group in ^{60}Ni. A corresponding level at 5.5 MeV in ^{58}Ni excited by alpha particles[3] has been assigned 4^+ with $\beta_4\approx0.06$. The ^{60}Ni group is in good agreement with this interpretation as $l=4$; however, the β_4 value required of 0.13 is rather large.

The relatively strong groups at 2.97 MeV in ^{54}Fe and 3.16 MeV in ^{56}Fe are assigned $l=2$ here. On the vibrational model these could be regarded as states of the two-quadrupole-phonon triplet, which would be excited with amplitudes second order in the deformation β_2. Both multiple (via the first 2^+ state) and direct excitation would contribute, but the calculated[14] cross sections are an order of magnitude smaller than those observed. Further, the excellent agreement in shape with the predictions of the first-order theory argues against a 2-phonon character for these states. At this energy, multiple excitation (on the vibrational model) is still about 2 or 3 times as intense as the direct, and has a quite different angular distribution. The measurements then indicate either considerable mixing between the 1- and 2-phonon states, or else quite a different interpretation for the second 2^+.

3. Average Optical Potential

It is believed that some of the fluctuations from nucleus to nucleus in the values of the optical parameters given in Table I are due to ambiguities in the fitting procedure as well as, perhaps, variations in the experimental data. For this reason, some effort was made to find a set of average values of the geometrical parameters which gave a good over-all fit to the scattering from Fe, Ni and Cu. No exhaustive study was made, but good results seem to be given by choosing $r_0=1.18$ F and $a=0.7$ F for the real potential, and with $a'=0.7$ F and $r_0'=1.04$ F (surface) or 1.40 F (volume) for the two types of absorptive potential. In addition, V_s was fixed at 7.5 MeV, since the scattering is insensitive to small changes in this parameter. With this choice, the optimum values of V and W or W_D were found for each nucleus, and are given in Table III. The predicted cross sections are compared to those of experiment in Fig. 9, and it is seen that the fits are quite comparable to those shown in earlier figures.

We were then tempted to try this set of parameters on the other data for 40-MeV proton scattering from ^{12}C, ^{27}Al, Sn, Ta, and Pb, again varying only V and W or W_D for optimum fits. The results are shown in Fig. 10; the agreement with experiment is remarkably good considering that this represents a large extrapolation beyond the mass region ($A\sim60$) from which the parameters were deduced. Theory shows stronger oscillations than experiment for Ta; this is almost certainly due to the large deformation of this nucleus which both allows quadrupole contributions to the elastic scattering and also gives low-lying excited states which are difficult to resolve experimentally. Perhaps most remarkable is the good account this potential gives of the scattering from ^{12}C; this is discussed further below. The data for Sn were reduced 15% in magnitude from those given in Ref. 7; these are within the experimental uncertainties and gave considerably better fits, particularly at forward angles.

We would not wish to suggest that this is the *optimum* set of parameters, even for the $A\sim60$ region. But at least it would seem to represent a good set of starting values in a search for a best fit to a particular set of data. The reaction cross sections given in Table III for the average geometries are close to those obtained with the best fits of Table I. However, an interesting feature is that now the real well depths V for Fe, Ni, and Cu show a tendency to *increase* with increasing asymmetry number $\epsilon=(N\text{-}Z)/A$, contrary to the radius-adjusted values for the best fits. This emphasizes the need for care when investigating some behavior which depends upon small changes in the parameter values. When the whole range of targets from C to Pb is considered, the increase with ϵ is clear. Because of the scatter in values

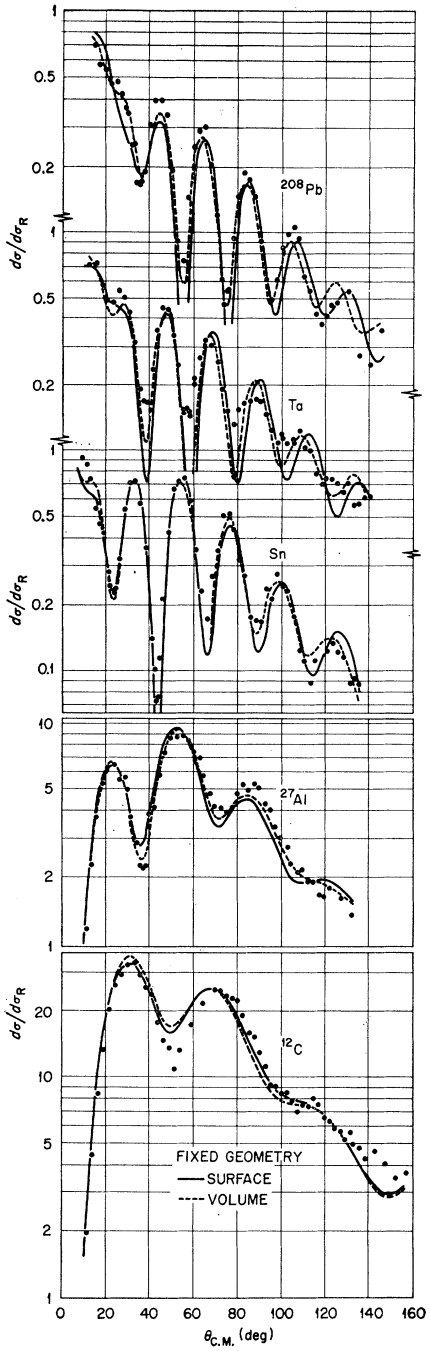

FIG. 10. Fits to elastic scattering from C, Al, Sn, Ta and Pb using potentials with the "average geometry." The calculations are made for both surface and volume forms of absorption with the parameters given in Table III.

of V it is not possible to give a definite figure for the coefficient of ϵ, but it does seem to be significantly larger than the value found at lower energies. (The variation of V with Z which arises because of its energy dependence has to be removed first. At lower energies this is believed to give a contribution to V of approximately $0.4Z/A^{1/3}$.)

The inelastic scattering was also calculated using the average-geometry potentials of Table III. Except for ^{58}Ni, the results are essentially identical to those shown in Figs. 2 through 6. The corresponding β values are included in Table II, and also agree well. The calculations for ^{58}Ni are shown in Fig. 11, and the fit, in the case of surface absorption, is in fact better than that shown in Fig. 4. We also note that the "best-fit" parameters for the ^{58}Ni-elastic data deviate the most from the average set. This may reflect a feature that has been found previously when analyzing inelastic or rearrangement collisions using the distorted-wave method. Namely, better results are often obtained by using optical parameters which give a good average fit to data for several adjacent nuclei than those which give the absolute best fit for a particular nucleus. The latter may reflect some idiosyncracies in the data.

Calculations were also made for the inelastic scattering to the 1.37-MeV 2^+ state in ^{24}Mg, using the average-potential parameters for ^{27}Al given in Table III. The results are compared to experiment in Fig. 12 for the volume-absorption potential; surface absorption gives essentially the same results. Again there is a small but definite improvement in fit when complex coupling is used.

4. The Target ^{12}C

Because it is such a light nucleus, some separate discussion of ^{12}C is appropriate. As we have already seen

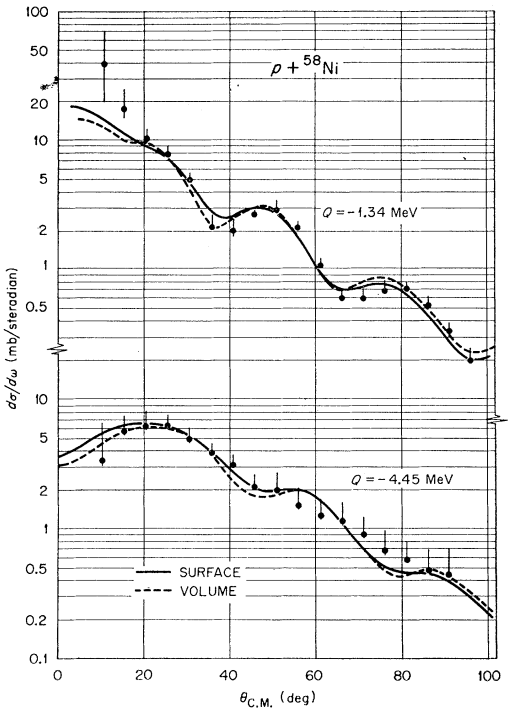

FIG. 11. Fits to inelastic scattering from ^{58}Ni using the "average-geometry" potentials of Table III. The calculations are made with complex coupling and include Coulomb excitation.

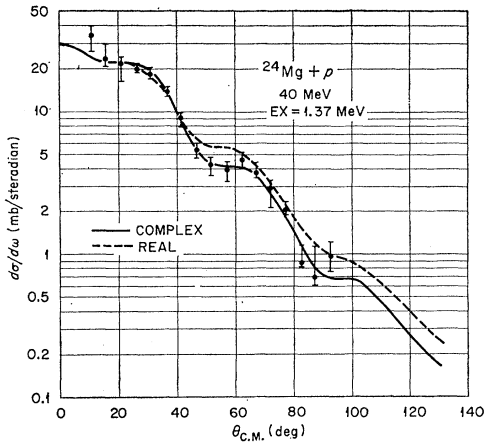

FIG. 12. Inelastic scattering from ^{24}Mg. Real- and complex-coupling calculations are shown which use the volume-absorption potential for ^{27}Al given in Table III (the surface-absorption results are essentially the same). β_2 for the real form factor is 10% higher than for the complex form factor.

(Fig. 10), the average geometry gives a good fit to the elastic scattering. When all seven parameters are varied for an optimum fit, both volume- and surface-absorption forms converge to a real potential with $V \approx 34$ MeV, $r_0 \approx 1.22$ F, $a \approx 0.67$ F, and $V_s \approx 7$ MeV. The volume imaginary potential tends to $W \sim 8$ MeV with a smaller radius, $r_0' \sim 1.0-1.2$ F, than the average geometry, but the values of r_0' and a' are very poorly determined. Similarly for the surface form; when a' is held fixed at 0.7 F, the radius converges to $r_0' \approx 0.75$ F with $W_D \approx 6$ MeV. However, when a' is varied also it takes the large value of 1.2 F while r_0' tends to zero with $W_D \approx 8$ MeV. At first sight these two results are very different, but both volume and surface forms have rather similar shapes, being peaked at the center of the nucleus and with a long tail. Although they give the lowest χ^2 values ($\chi^2 \approx 2$), subjectively there is little to choose between these fits and those obtained when the average geometry is used for the imaginary potential. Figure 13 shows the results of using the average imaginary geometries and the optimum real geometry of $r_0 = 1.22$ F, $a = 0.67$ F. The best well depths were then $V = 34.5$ MeV, $W = 4.9$ MeV (volume, $\chi^2 = 3.2$) or $V = 35.3$ MeV, $W_D = 4.2$ MeV (surface, $\chi^2 = 5.4$).

Calculations of the inelastic scattering for $l = 0$, 2 and 3 were remarkably insensitive to the potentials used, all giving closely similar results. Further, the differences between predictions with complex and real coupling are quite small in this case, because the absorptive potential is relatively weak. In no case is the observed rise in the 2^+ cross section at back angles reproduced by the theory. Because of the possibility that this arose from higher-order coupling effects which are not included in the distorted-wave approximation, some calculations were made solving explicitly the coupled equations for the ground and 2^+ states. An automatic search routine was used to optimize the fit to the elastic and 2^+ inelastic data simultaneously.[14] First, searches were carried out retaining the collective-model prescription for the coupling form factor (3), but no improvements resulted; higher order effects of the coupling are negligible. Then the routine was used to study variations in the coupling form factor. The real form (3) was used except that the diffuseness parameter a_{EX} for $r > R_0 = r_0 A^{1/3}$ was allowed to differ from that a_{IN} for $r \leq R_0$, so that asymmetrically-shaped form factors are allowed.

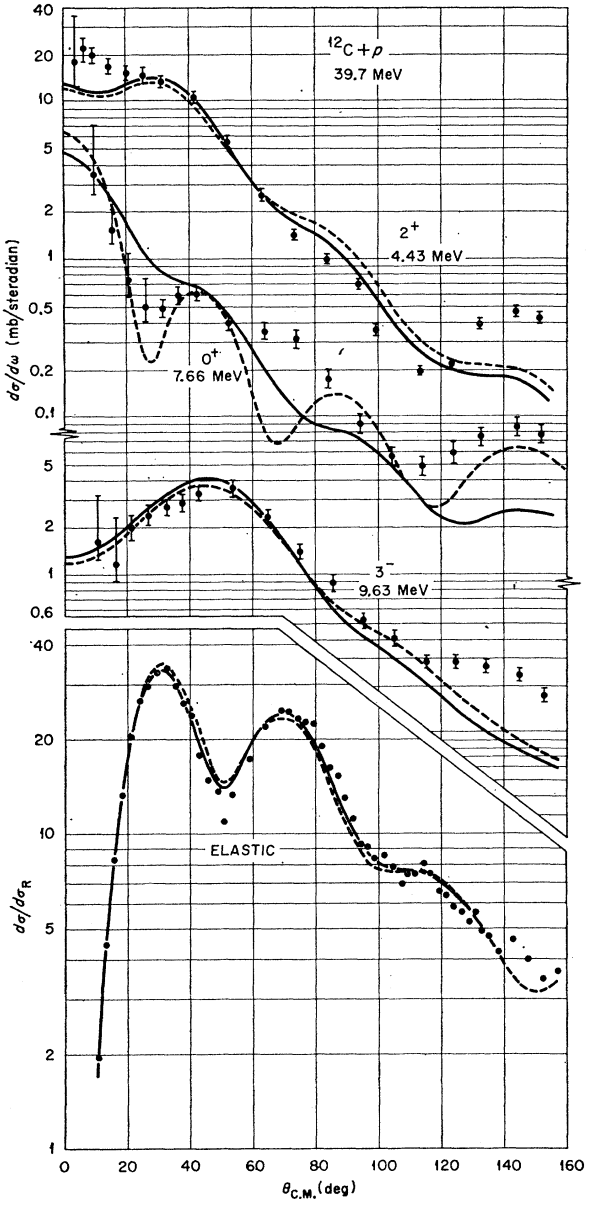

FIG. 13. Scattering from ^{12}C. The elastic-scattering curves are for the "best-fit" surface-(full line) and volume-(dashed) absorption potentials described in the text. The inelastic scattering was calculated with the surface form; the results for volume absorption are nearly identical. The full curves are for complex coupling, while the dashed curves for the 2^+ and 3^- are for real coupling. The dashed curve for $l = 0$ is discussed in the text.

The parameters R_0, a_{EX} and a_{IN} were then treated as independent, no longer tied to the optical potentials used, and were varied to optimize the fit to the inelastic-scattering data. Again no improvement resulted; the optimum values did not differ significantly from the optical-potential values. In view of this, it appears that new interaction features have to be introduced if the fit to the 2^+ scattering is to be improved; one possibility is a spin-flip term.

The fit to the 3^- cross section is reasonable, although again there are discrepancies at back angles. The 0^+ cross section is only reproduced qualitatively by using the form factor (3) (solid curve in Fig. 13). This form factor is appropriate to a simple dilatational or "breathing-mode" vibration, in which the radius R of the potential well is changed to $R(1+\beta_0)$ without change in depth. One might expect the depth to decrease as the nucleus expands, and this would add a volume term to the coupling interaction. Doing this, however, worsens the agreement with the angular distribution of the measured inelastic scattering.

We might also consider an interaction whose form factor was concentrated in the surface but changed sign there. An oscillation in the magnitude of the surface diffuseness would give such an interaction. As a crude indication of the consequences of this, the cross section was calculated assuming that the nuclear matrix element had the form $vh(r)$, where

$$h(r)=(d^2/dx^2)[(e^x+1)^{-1}]$$

and x is given by Eq. (1), $x=(r-2.793)/0.67$. This gives the dashed curve in Fig. 13, normalized with $|v|=41$ MeV; the structure of the angular distribution is in much better agreement with the experiment. It seems that an interaction with a node in its radial distribution is required to reproduce this structure.

IV. SHELL MODEL

As an alternative to the collective-model interaction used in the work presented here, we might consider using shell-model wave functions and allowing the projectile to interact with each target nucleon through an effective two-body potential. Of the nuclei studied here, ^{54}Fe is particularly suitable for such a microscopic description because the neutron $1f_{7/2}$ shell is filled and the low states may be regarded as due to the two $1f_{7/2}$ proton holes. This model has been used by Funsten *et al.*[2] for an analysis of proton scattering at 18 MeV from ^{54}Fe and other $N=28$ nuclei, using a central Gaussian interaction

$$v(r)=-V_0\exp(-\gamma r^2)$$

between the projectile and each target nucleon. At that energy it is found that the angular distributions predicted are relatively insensitive to the interaction model (collective or shell), being determined largely by the l transfer and the optical distortion. We have made similar calculations for ^{54}Fe at 40 MeV both with the Gaussian and with a Yukawa potential[25]; the differential cross sections are now a little more sensitive to the radial dependence of the interaction. Using the same range ($\gamma=0.293$ F^{-2}) as Funsten *et al.*,[2] we find an $l=2$ angular distribution which does not fall off as rapidly with angle as the observed 1.34-MeV group. This property varies somewhat with the range γ, and further studies are under way to determine the optimum value of this parameter. The strength required, $V_0\approx 40$ MeV, is of the same order as that found at the lower energy.

V. CONCLUSIONS

The optical model, with surface or volume forms of absorptive potential, has been found to give a very good account of the present elastic-scattering data. It is not possible to choose between volume and surface forms on the basis of differential or absorption cross sections alone, at this energy .The radius and diffuseness parameters needed here (Table I) definitely differ from the values suggested by analyses of lower energy (9-22 MeV) data. However, it is possible that the values deduced at 40 MeV would be equally acceptable at the lower energies.

The calculated inelastic scattering is equally insensitive to the choice of surface or volume absorption. The collective-model interaction, obtained by deforming the optical potential, is found to reproduce the observed angular distributions very well, provided both real and imaginary parts of the potential are deformed. The identifications of multipole order are readily made, particularly from the forward-angle behavior of the data (see Fig. 1). The deformation parameters β_l needed to reproduce the magnitudes of the observed cross sections (Table II) are in good agreement with those obtained by other experiments. The values of β_l given here are those obtained with complex coupling. Within a 10% uncertainty in judging normalization, the same values were found with any of the options discussed. The difference in β_l found with surface or volume absorption did not exceed 10% for any case; nor was the difference any larger between values found with the potentials of Table I or Table III. For any given potential, the real-coupling value required for β_l was consistently about 10% larger than the complex-coupling value.

ACKNOWLEDGMENTS

We are particularly indebted to R. H. Bassel and R. M. Drisko for numerous acts of assistance and helpful discussions during the course of this work. We are also grateful to B. Buck for making available the coupled-equations code.

[25] The interaction form factors were computed using a code written by L. W. Owen and M. B. Johnson at ORNL, assuming that the protons are bound by 8 MeV in a Saxon-Woods potential with the same parameters as those that fit the elastic scattering.